Neoplasia • Vol. 6, No. 5, September/October 2004, pp. 490–502 490

www.neoplasia.com

# Gene Expression Profiling of Mouse Teratocarcinomas Uncovers Epigenetic Changes Associated with the Transformation of Mouse Embryonic Stem Cells

*Allison E. Bonner*, Yian Wang† and Ming You†*

*Division of Human Cancer Genetics, The Ohio State University Comprehensive Cancer Center, 420 West 12th Avenue, Columbus, OH 43210, USA; †Department of Surgery and The Alvin J. Siteman Cancer Center, Campus Box 8109, Washington University School of Medicine, St. Louis, MO 63110, USA

**Abstract**

**The molecular mechanisms of the development of teratocarcinomas from stem cells are largely unknown. To determine which genes are associated with the transformation of these cells, we have performed oligonucleotide microarray analysis, using Affymetrix U74A GeneChips, on both cell cultures and tumors in nude mice. We identified 68 genes that significantly differed in expression between the ES cell culture and the teratocarcinoma cell line, SCC-PSA1, and 51 genes with statistically different expression patterns between the ES cell tumors and the teratocarcinomas ($P < .00005$). We found that there were 20 genes that had common expression patterns in both groups. We also examined the role of the transition from *in vitro* to *in vivo* by comparing ES cell culture to ES cell tumor, and teratocarcinoma cell line to teratocarcinomas. We identified 22 genes that were upregulated in the ES cell tumors and 42 that had a decreased expression in the tumor ($P < .0001$). In comparing SCC-PSA1 to its tumor, we identified 34 upregulated genes and 25 downregulated genes ($P < .001$). There were only 10 genes in common from these two lists. GenMapp search revealed that several pathways, especially the cell cycle pathway, are actively involved in the induction of teratocarcinomas. Our results indicate that many key development genes may play a key role in the transformation of ES cells into teratocarcinoma cells.**

*Neoplasia* (2004) **6**, 490–502

**Keywords:** Teratocarcinoma, microarray, ES cells, mouse, transformation.

## Introduction

Cancer is a complicated and heterogeneous disease, taking many forms and affecting many tissues. Dysregulation of the cell cycle is a common factor among all types of cancer. The ability to activate alternative pathways to regain cell cycle control, or stimulate apoptosis after some form of cellular damage, would be a valuable way to fight cancer. Developmental genes are strict regulators of cell cycle and apoptosis; therefore, the genetic components of embryonic development are potential sources of cancer phenotype rescue. They are responsible for the migration and differentiation of all of the body's cell types, as well as for the maintenance of appropriate cell mass (i.e., apoptosis). These genes have the potential to override the signals sent by the cancer cells' abnormal gene expression and are therefore excellent candidates for gene-based therapies.

In order to study developmental gene regulation in the context of carcinogenesis, we have undertaken the physical and molecular characterization of teratocarcinomas. Teratocarcinomas are embryonic cancers that are most often found in the sex organs of human adults, but they have been seen in various locations throughout the body in patients. In adult humans, spontaneous teratocarcinomas originate primarily from germ cells, but teratocarcinomas can also form from dysregulated stem cells, which are most frequently seen in prenatal or newborn tumors. Characteristic morphology of teratocarcinoma tumors includes diploid embryonic stem cells mingled with immature tissues and highly specific, differentiated tissue (e.g., muscle, bone, teeth, etc.) [1].

The objective of this study was to determine the possible mechanisms that dictate the tumorigenic properties of teratocarcinomas by comparing them to their embryonic stem cell progenitors. By using oligonucleotide array analysis, we can observe the repercussions of carcinogenic transformation by examining gene expression changes between the teratocarcinoma and the embryonic stem cell control. We examined cultures of these two cell types, as well as tumors in nude mice, in order to elucidate the mechanisms of tumorigenic properties of teratocarcinomas. The results from this study have the potential to shed new light on mechanisms of carcinogenesis.

Address all correspondence to: Ming You, Department of Surgery and The Alvin J. Siteman Cancer Center, Campus Box 8109, Washington University School of Medicine, 660 S. Euclid Avenue, St. Louis, MO 63110. E-mail: youm@msnotes.wustl.edu

Received 15 January 2004; Revised 6 March 2004; Accepted 8 March 2004.



DOI 10.1593/neo.04124

## Materials and Methods

### *Teratocarcinoma and ES Cells*

The experiments described in this paper were performed using the following cell lines and conditions. An established murine diploid teratocarcinoma cell line, SCC-PSA1, was obtained from the American Type Culture Collection (ATCC; Manassas, VA). Cells were grown in DMEM media (Gibco, Grand Island, NY) containing 10% fetal bovine serum (FBS) (147; Gibco) and 1% penicillin/streptomycin (Gibco) at 37°C in 5% $CO_2$. The teratocarcinoma cells were grown on feeder layers of STO cells (ATCC) that had been treated with 10 μg/ml mitomycin C (Sigma, St. Louis, MO) for 6 hours. The TC1 ES cell line was obtained from the laboratory of Michael Weinstein (Ohio State University, Columbus, OH). The ES cells were grown on STO feeder layers in the same conditions as described above using DMEM media containing 15% FBS, 1% penicillin/streptomycin 1% MEM nonessential amino acids (Gibco), 1% L-glutamine (Gibco), 500 μl of leukemia-inhibitory factor (LIF; ESGRO, ESG1106; Chemicon International, Temecula, CA), and 4 μl of β-mercaptoethanol (Sigma). Both the SCC-PSA1 cell line [2] and the TC1 cell line were derived from 129Sv mice.

### *Tumor Induction*

Tumors were induced in inbred BALB/c athymic nude mice (BABL/cAnNCrj-nu; Charles River, Wilmington, MA). Mice, receiving 500,000 teratocarcinoma and control ES cells, were injected with teratocarcinoma cells on the right flank and control ES cells on their left flank. Four mice were used in this study. Tumor latency and volume ($cm^3$) were monitored over a period of 45 days. At the conclusion of that period, the mice were sacrificed and the tumors were measured and weighed. Any test animal whose tumor size imposed too great a burden was sacrificed prior to the end of the study.

### *Cytogenetics*

After treatment with Colcemid at a concentration of 10 μg/ml in Hanks' balanced salt solution (Gibco) for 30 minutes, the hypotonic solution potassium chloride (KCl) was applied at 0.075M for 20 minutes (Sigma), followed by the fixative Carnoy's solution [methanol (Fisher, Fairland, NJ):glacial acetic acid 3:1] overnight. The samples were then dropped on clean microscope slides and stained with Wright stain. After overnight desiccation, the cells were examined for chromosomal abnormalities by light microscopy ($\times$ 40 – $\times$ 100). Two cells from 10 different slides were examined in order to determine a representative population.

### *RNA Amplification*

Total cellular RNA was collected from each time point. Total RNA was isolated by Trizol (Invitrogen, Carlsbad, CA) and was cleaned up with a Qiagen RNeasy Mini kit (QIAGEN, Valencia, CA). *In vitro* transcription-based RNA amplification was then performed on each sample. cDNA was synthesized using the T7-(dT)24 primer: 5′-GGCCAGTGAATTGTAATACGACT-CACTATAGGGA6GCGG-(dT)24-3′. The cDNA was cleaned using phase-lock gel (Fisher) phenol/chloroform extraction. After clean up, *in vitro* transcription labeling was performed using the Enzo "Bioarray Kit" (Affymetrix, Santa Clara, CA). The resulting cRNA was cleaned up, again using the Qiagen RNeasy Mini kit.

### *Affymetrix GeneChips Probe Array*

Affymetrix Mu74Av2 GeneChips, encompassing ~12,000 genes and expressed sequence tags (ESTs) on one array, were processed according to the manufacturer's recommendations. Approximately 16 probe pairs (oligonucleotides) represent every gene or EST in a probe set. One sequence represents the complimentary strand of the target sequence, whereas the other has a 1-bp mismatch at the central base pair position. This mismatch sequence serves as an internal control for specificity of hybridization. The relative expression is reported as the average difference of the fluorescence intensity values between the perfect match and the mismatch oligonucleotides, resulting in the "average difference" value [3,4].

### *Statistical Analysis*

Four independent samples were collected per time point. Stages of analysis consisted of: 1) array normalization; 2) estimation of gene expression; and 3) statistical testing. To make arrays comparable, raw intensity values within CEL files were normalized by regression as follows. A pseudo-array was produced, consisting of the median spot intensity determined across all arrays for all spots. Each real array was quadratically regressed against this median pseudo-array. Resulting scaled CEL files were used to estimate gene expression according to the full model index of Li and Wong (LWF), which was recently shown by Lemon et al. [5] to be superior to both the Li–Wong reduced model and Affymetrix average difference [6]. Genes with negative expression indexes were removed.

In order to determine expression change, a standard Student's *t* test was performed between the average values for each group based on the analyses desired (e.g., ES cells in culture *versus* induced ES cell tumor). Genes selected for further study had a $P$ value <.0001 or .0005, depending on the group examined (see text). For the selected genes, expression indexes were transformed across samples to a $N(0,1)$ distribution using a standard statistical $Z$-transform. These values were input to the GeneCluster program and genes were hierarchically clustered using average linkage and correlation dissimilarity.

### *GenMapp*

Signal transduction pathways, metabolic pathways, and other functional groupings of genes were evaluated for differential regulation using the visualization tool GenMAPP (UCSF, www.genmapp.org). GenMAPP is a recently reported tool for visualizing expression data in the context of biologic pathways [7]. We imported the statistical results of our data set into the program and used GenMAPP to illustrate pathways containing differentially expressed genes. Differential gene expression was based on ES

tumors *versus* teratocarcinomas expression change (fold ± 1.5 and $P \leq .05$ as indicated by asterisk in Figure 7).

*Real-Time Polymerase Chain Reaction (PCR)*

Two micrograms of total RNA per sample, collected as described above, was converted to cDNA using the SuperScript First-Strand Synthesis system for real-time PCR (Invitrogen, Carlsbad, CA). The primer used to generate cDNA was the same as that used to generate cDNA for the oligonucleotide array assay [T7- $(dT)_{24}$ primer: 5′-GGCCAGTGAATTGTAATACGACTCACTATAGGGAGGCGG-$(dT)_{24}$-3′]. cDNA generated from each of the samples comprising one group was then pooled and real-time PCR was performed.

The real-time PCR assay was performed using the Bio-Rad iQ SYBR Green Super Mix kit (BioRad, Hercules, CA). The following primers were used to amplify the genes of interest: CDC7 F-ACTGCAGTTTCTGGGTGCTT, R-AGCAGGAACTCCTCAGCAAG; clusterin F-TGTGGACTGTTCAACCAACAA, R-ATTCCCTCCCAGACACTCCT; disabled 2 F-GAGGAGCGGCTACCTTTACC, R-GGTCAAACAGCTGCAACGTA; MAD2 F-GCCGAGTTTTTCTCATTTGG, R-CCGATTCTTCCCACTTTTCA; MFAP2 F-GAGGAACTTCTCCGAGCTGA, R-AAAACAGAGGTGGTCCATGC; PEM F-AAATGGAGGAAAAGGCCACT, R-TTCTCCCCATCTCACTCCAC; trophoblast glycoprotein F-CAACCTGACACACCTCGAAA, R-GGTCCGCATTGATTTCGTAT. One microliter of pooled cDNA was added to a 25-μl total volume reaction mixture containing water, iQ SYBR Green Super mix, and primers. Each real-time assay was performed in triplicate. Data were collected and analyzed on the BioRad iCycler version 2.033. GAPDH (primers: F-TGGAGAAACCTGCCAAGTATG, R-GTGGGTGCAGCGAACTTTAT) was used as an internal standard. The GAPDH value, a reflection of the number of cycles needed to reach a threshold of fluorescence, was subtracted from the cycle value for the individual gene whose expression was being assessed. Fold change was assessed by dividing the microarray expression value or the real-time expression value for the cancerous tissues by the values generated for the age-matched control tissues. For the calculation of the fold-change values in Figure 4, the age-matched sample N1 was used for the control value for the ADE sample and the age-matched sample N2 was used as the control value for the CAR sample.

## Results

In our search to better define the tumorigenic properties of teratocarcinomas, we have characterized the properties of teratocarcinoma cells. The basic morphology of teratocarcinoma cells in culture is quite similar to ES cells (data not shown), complicating the differentiation between the two cell types. When kept in media that contains LIF and on a bed of feeder cells, such as mitomycin C–treated STO cells, ES cells maintain a slightly clumped distribution across the surface of the cell culture plate and have a round shiny appearance. This is also the case for teratocarcinoma cells, but the addition of LIF is not necessary to maintain the undifferentiated state. One main difference between the two cell types is adherence. Teratocarcinoma cells are much less adherent to the feeder cell layer than the ES cells, making separation of teratocarcinoma cells from the feeder layer much easier.

Although the growth of ES cells and teratocarcinoma cells is relatively similar *in vitro*, growth *in vivo* is quite different. Figure 1 shows the growth differences of the teratocarcinoma cells *versus* the ES cells. Three nude mice were injected with $5 \times 10^5$ ES cells on the left flank and $5 \times 10^5$ teratocarcinoma cells on the right flank. In Figure 1*A*, an *in situ* picture of representative tumors from the nude mice injections is presented. In Figure 1*B*, the tumors from Figure 1*A* have been excised and the size is shown with a metric ruler. Figure 1*C* is a graph detailing the tumor weight differences between the average of the ES cell tumors and the teratocarcinoma tumors ($P < .05$). It is clear from this figure that teratocarcinoma cells grow at a much faster rate than the ES cells.

Morphology of the two tumors was also similar to a point. Both cell types resulted in tumors with differentiated tissues, including skeletal muscle, squamous epithelium, and vascular tissues, as seen in Figure 1, *D* and *E*. In the ES cell benign tumors, vasculature was restricted, whereas in the teratocarcinomas, extensive recruitment of blood vessels was seen. The major defining characteristics of the teratocarcinomas were the extensive areas of necrosis and frequent mitotic figures, leading to the conclusion that the teratocarcinoma tumors have metastatic capabilities. There are also several other tissue types present in the teratocarcinomas, such as cartilage and glandular materials, that were not seen in the ES cell tumors.

In order to better characterize the teratocarcinoma cell line, SCC-PSA 1, we undertook cytogenetic analysis to determine whether or not large chromosomal abnormalities were responsible for the phenotypic changes seen between the ES cells and the teratocarcinoma cells. The common karyotyping method of G-banding using trypsin and Wright's stain (GTW) was applied to two separate cultures of the SCC-PSA 1 cell line. Of the 20 separate metaphase spreads identified, the normal murine diploid karyotype number of 38 autosomes and 2 sex chromosomes, in this case two X chromosomes, were seen in each cell. Figure 2 is a representative metaphase spread (*A*) and karyotype (*B*) of the SCC-PSA 1 cell line. Because the computer program used to assist in the karyotyping was designed for human karyotypes, there are several extra numbers associated with the figure that do not correspond to murine chromosomes.

Because there were no major chromosomal abnormalities detected in the 20 cells that were examined by karyotyping, we hypothesize that other genetic changes are responsible for the phenotype differences between ES cells and teratocarcinoma cells. In order to assess the genetic changes occurring during the transition from ES cell to teratocarcinoma cell, we used Affymetrix U74A GeneChips microarrays to determine the overall gene expression changes between both ES cell cultures and tumors, and

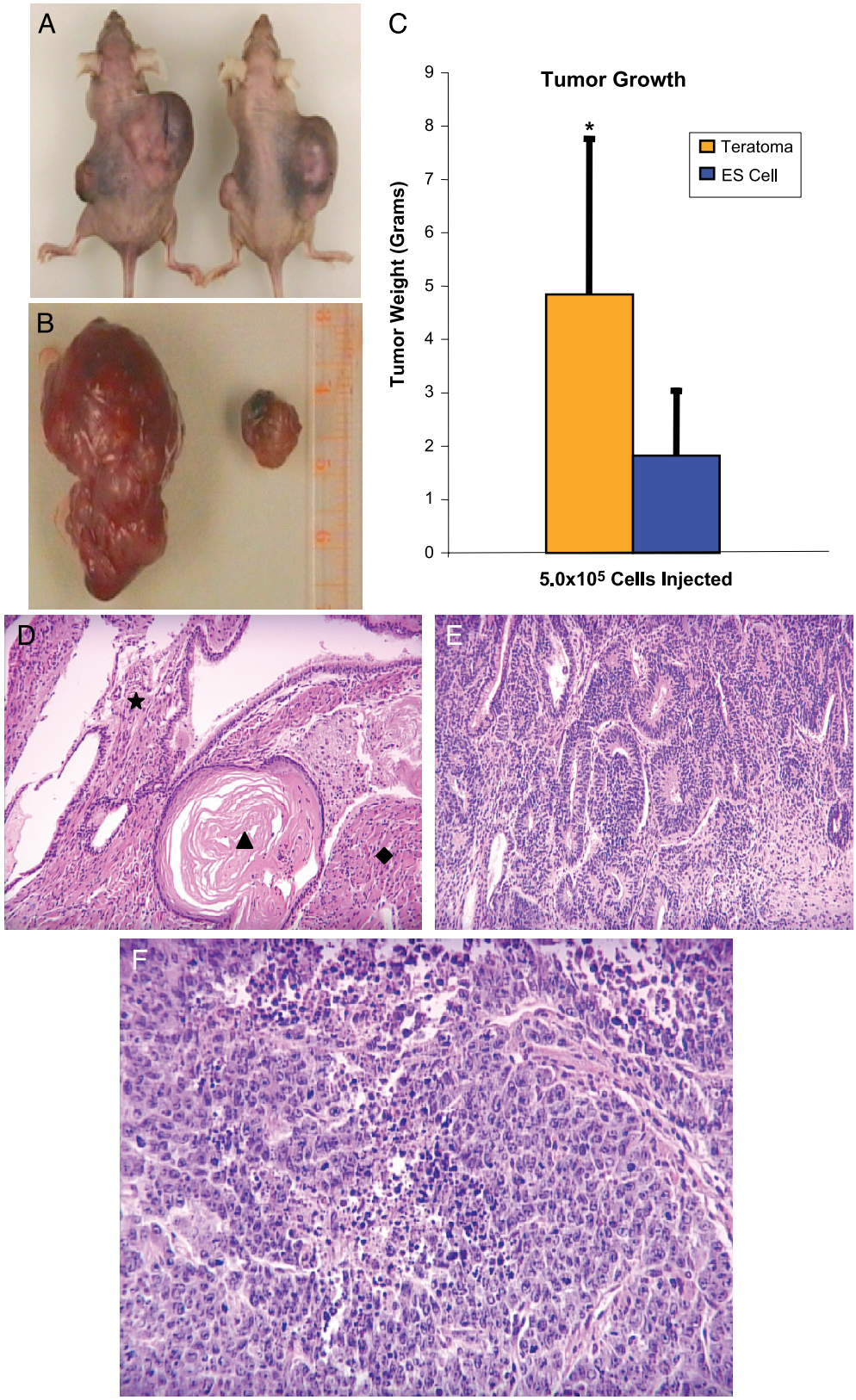


**Figure 1.** *Characterization of teratocarcinoma tumor growth referenced to ES cell tumor growth. (A) Representative tumors in situ. About 5 × $10^5$ ES cells were injected on the left flank of the mice and 5 × $10^5$ SCC-PSA1 (teratocarcinoma) cells were injected on the right flank. (B) Resected tumors. Representative tumors from the nude mouse experiment were resected and photographed. Centimeter ruler to the right to indicate tumor size. (C) Differential growth of the ES cell tumors and teratocarcinomas ($P < .05$). The orange bar represents average teratocarcinoma growth; the blue bar represents ES cell growth. Tumor weight in grams is on the Y-axis. (D) Hematoxylin and eosin (H&E) staining of section of resected tumors. This area demonstrates the tissue types of (★) glandular epithelium, (▲) squamous epithelium, and (◆) mature skeletal tissues, which were similar in both the ES cell tumors and the teratocarcinomas. (E) H&E staining of another portion of tissue, immature neuroepithelial rosettes, similar in both tumor types. (F) H&E–stained section from a teratocarcinoma demonstrating the areas of necrosis and frequent mitotic figures, which is unique to the teratocarcinomas.*

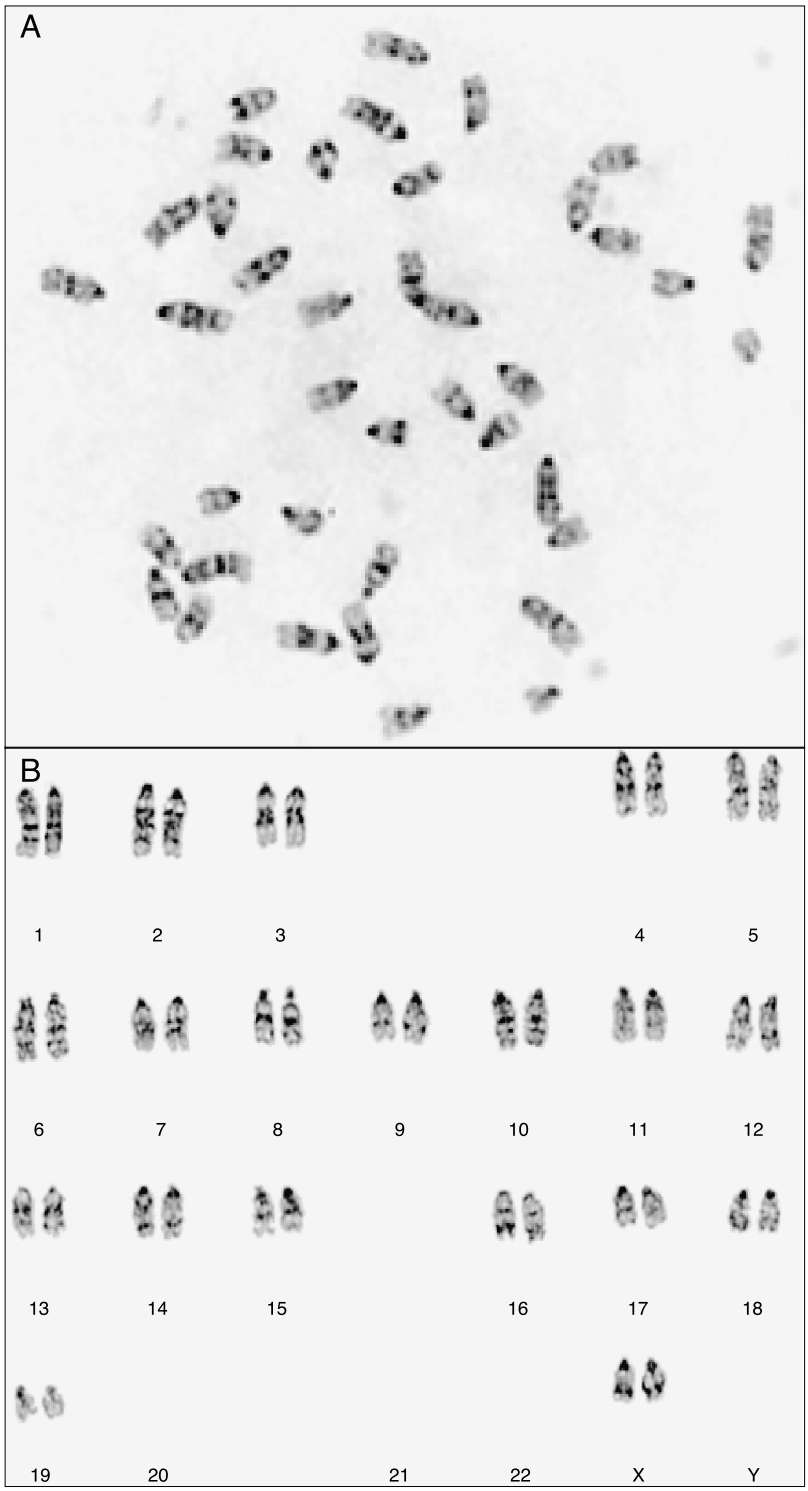


**Figure 2.** *Karyotype analysis of SCC-PSA1 cell line. (A) Representative metaphase spread for the SCC-PSA1 cell line. Twenty separate metaphase spreads were examined and no detectable numerical abnormalities were found. (B) Representative karyotype of SCC-PSA1 cell line. A normal karyotype of 38 autosomes and 2 sex chromosomes was seen in all 20 of the cells examined. No apparent chromosomal abnormalities were identified. Note: The computer program used to display the karyotype is intended for human karyotypes, leading to the excess of numbers that do not correspond to any murine chromosomes.*

teratocarcinoma cell cultures and tumors. Total RNA was isolated from ES cell and teratocarcinoma cell cultures 2 days after plating, as well as from flash frozen portions of the resected nude mouse ES and teratocarcinoma tumors. Analysis of expression included a two-tailed Student's *t* test as well as fold-change detection.

In order to better understand the mechanisms of tumorigenesis, we examined the gene expression changes between the ES cell cultures and the teratocarcinoma cell cultures, as well as the gene expression changes between the ES cell tumors and the teratocarcinomas from the nude mice study. Figure 3 contains two lists, detailing the genes

with a *P* value of less than .00005 for both of the analyses. Figure 3*A* contains data for the cell culture comparisons, 68 total genes with 28 upregulated in the teratocarcinoma cell culture and 40 genes downregulated in the teratocarcinoma cell culture. Figure 3*B* contains the tumor data, displaying 31 genes upregulated in the teratocarcinoma tumor and 20 genes downregulated. There are several genes of interest whose expression is significantly altered in the teratocarcinoma cell cultures. Increased expression is seen in MCM 4, a critical factor in DNA replication, as well as the c-myc–responsive gene, *JPO1*. As would be expected, teratocarcinoma-derived growth factor expression is increased, as is the expression of the Bloom syndrome gene.

Interestingly, Ras 1 expression and *GRO1* expression are significantly decreased in the tumor cell line. We do see decreases in the anti–proliferative factor B-cell translocation 1 and GATA-6, usually associated with lung cell differentiation. Clusterin, a controversial protein found to both inhibit and encourage apoptosis, has decreased expression as well. Finally, HMG2, a cellular differentiation factor, is also decreased.

Between the ES cell tumor and the teratocarcinoma, there are also some very interesting expression changes. Both CDC 25 and CDC 7, critical factors in cell cycle progression, are overexpressed in the teratocarcinomas. The homologue of the human *Highly Expressed in Cancer* (*HEC*) gene is predictably overexpressed as well. ADAM 8, a cell adhesion molecule, is significantly downregulated in the teratocarcinoma, possibly allowing for local tissue invasion. Calcyclin, usually seen to be upregulated in cancers such as prostate, is decreased in the teratocarcinoma in our study.

To exclude genes whose expression changes might be the result of the environment change (i.e., from *in vitro* to *in vivo*), we examined the cell types in relation to each other. Figure 4 lists the genes whose change in expression between the cell culture samples *versus* the tumor has a *P* value of less than .0001. Figure 4*A* compares ES cells in culture to the ES cell tumors induced in nude mice, and Figure 4*B* compares teratocarcinoma cells in culture to the teratocarcinoma tumors induced in nude mice.

Between the transition from *in vitro* to *in vivo* for the ES cells (Figure 4*A*), we see 64 genes with significant expression changes. The 42 genes downregulated in the ES cell tumor include the key cell cycle regulators CDC2A, CDC6, and cyclins B1 and F. Interestingly, we also see downregulation of several known oncogenes: placentae and embryos oncofetal gene (*PEM*), *HEC*, and *GRO1*. This has interesting implications in respect to the conditions of cell culture and its effect on the cell.

There are relatively fewer genes upregulated in the ES cell tumor. We do see two known oncogenes upregulated in the ES cell tumors, E26 avian leukemia oncogene 1 (Ets1) and lung carcinoma myc-related oncogene 1. Heat shock proteins 2 and 40B10 are also upregulated in the ES cell tumor.

There are 59 genes with significant expression changes found between the teratocarcinoma cell line and the teratocarcinoma tumor (shown in Figure 4*B*)—34 with an increased expression in the tumor and 25 downregulated in the tumor. The BCL2-related protein A1D is upregulated in the teratocarcinoma, as is Rho B. Hepatocellular carcinoma–associated antigen 112 is also upregulated in the teratocarcinoma.

As was seen in the ES cell tumor, PEM is downregulated in the teratocarcinoma. Embryonal stem cell–specific 1 is downregulated as well, implying in the name that the teratocarcinoma is clearly a different cell type than the ES cell from which it is derived. Along those same lines, undifferentiated embryonic cell transcription factor 1 also has decreased expression in the tumor, alluding to the potential for differentiation that is the hallmark of the teratocarcinoma phenotype in humans.

GenMapp search revealed that the cell cycle pathway is actively involved in the development of teratocarcinomas with changes in multiple cell cycle genes (*BUB1*, *MAD2L1*, *Cdc25A*, *Cdh1*, *CycB1*, *CDK1*, *WEE1*, *Cdc7*, *DP1*, *CDK4*, *MCMs*, and *E2F5*) (Figure 7). Several cellular pathways–related genes are also found including apoptosis (caspase 3, caspase 7, poly [ADP ribose] polymerase-1), TGFβ pathway (thrombospondin, Smad2, 5′-TG-3′ interacting factor), and Wnt pathway (wnt-4, wnt-5a).

Our microarray results clearly demonstrate the genetic differences between embryonic stem cells and teratocarcinomas. In order to verify these results, we selected a subset of genes from all of the groups analyzed and performed real-time reverse transcription polymerase chain reaction (RT-PCR) to assess whether or not gene expression data from the microarrays was an accurate depiction of the transcription taking place. Figure 5 is a graphic representation of fold change between both the ES cell culture and teratocarcinoma cell culture data, and between the ES cell tumors and teratocarcinomas induced in nude mice. Although the fold change values for the comparisons between either group may differ, the expression patterns seen with the real time RT-PCR verify our microarray data.

## Discussion

In this study, we have characterized the tumorigenic properties and gene expression profiles of teratocarcinomas, which will further the understanding of teratocarcinoma development. We began our molecular characterization of teratocarcinomas based on the lack of evidence supporting large chromosomal abnormalities as a factor of tumorigenesis. We utilized microarray technology to observe the overall differences in gene expression that could be responsible for the teratocarcinoma phenotype. In order to understand the molecular processes that are contributing the most to the transformation of the ES cell into a teratocarcinoma cell, we have compiled a list of those genes whose expression pattern changes were common to both the cell cultures and the tumors. Figure 6*A* is a list of genes that the analyses from Figure 3 have in common ($P < .001$). There are 12 genes whose expression is increased in both the teratocarcinoma cell line and the teratocarcinoma, and eight genes whose expression is decreased in both sample types. All of the genes represented in this figure have a *P* value of less than

A

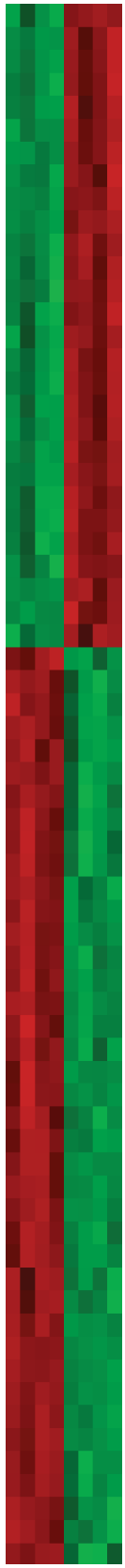


| Gene | FC | Probe ID | Pub Acc |
|---|---|---|---|
| Erythroid Differentiation Regulator | 1.68 | 98525_f_at | AJ007909 |
| Ectodermal-neural Cortex 1 | 2.60 | 98524_f_at | AI848479 |
| Ribonucleotide Reductase M2 | 2.17 | 102001_at | M14223 |
| Single-stranded DNA BP 1 | 1.57 | 100957_at | AA881160 |
| Mini Chromosome Maintenance Deficient 4 | 1.61 | 93041_at | D26089 |
| Undifferentiated Embryonic Cell TF 1 | 2.14 | 102220_at | AB017360 |
| Branched Chain Aminotransferase 2 | 2.12 | 100443_at | AF031467 |
| JPO1 | 1.85 | 95063_at | AI606257 |
| Small Nuclear Ribonucleoprotein N | 3.68 | 102163_at | X60388 |
| Solute Carrier Family 7-7 | 1.99 | 103818_at | AJ012754 |
| Folate Receptor 1 | 1.57 | 93785_at | M64782 |
| Branched Chain Aminotransferase 1 | 1.56 | 100026_at | U42443 |
| Aldo-keto Reductase 1-B3 | 1.87 | 162341_r_at | AV133992 |
| BRG1/brm-associated Factor 53A | 1.49 | 95659_at | AF041476 |
| Makorin 1 | 1.62 | 101069_g_at | AA656621 |
| Phosphofructokinase | 2.22 | 97834_g_at | AI853802 |
| Teratocarcinoma-Derived Growth Factor | 2.13 | 93002_r_at | M87321 |
| Ring Finger Protein 1 | 1.67 | 101068_at | AA656621 |
| Myo-inositol 1-phosphate Synthase A1 | 2.67 | 160337_at | AI847162 |
| Zinc Finger Protein 5 | 1.71 | 103989_at | AI314715 |
| Induced in Fatty Liver Dystrophy 2 | 1.15 | 161067_at | AA770736 |
| Eukaryotic Translation Initiation Factor 4E BP 1 | 1.32 | 100636_at | U28656 |
| Helicase | 1.63 | 93228_at | U25691 |
| Protein Typrotein Tyrosine Kinase 9 | 1.51 | 94020_at | Y17808 |
| Bloom Syndrome | 1.28 | 102631_at | AB008674 |
| Gastrulation Brain Homeobox 2 | 2.06 | 94200_at | Z48800 |
| Nuclear Protein 1 | 1.60 | 160108_at | AI852641 |
| Paternally Expressed 3 | 1.48 | 96765_at | AW120874 |
| Methionine Adenosyltransferase II alpha | 1.42 | 160362_at | AW124835 |
| Ephrin B2 | 1.84 | 160857_at | U30244 |
| Proliferin 2 | 2.36 | 93883_at | K03235 |
| B-cell Translocation 1 | 1.94 | 93104_at | Z16410 |
| Protein Tyrosine Phosphatase 16 | 1.51 | 104598_at | X61940 |
| Cartilage Associated Protein | 1.67 | 103817_at | AJ006469 |
| 3-O-sulfotransferase 1 | 2.37 | 102410_at | AF019385 |
| 2-cell-stage 1 | 1.46 | 96584_f_at | AF067060 |
| APR-3/p18 | 1.83 | 160271_at | AW121255 |
| FBJ Osteosarcoma Oncogene | 2.53 | 160901_at | V00727 |
| Rho-guanine Nucleotide Exchange Factor | 1.86 | 92710_at | U73199 |
| Eukaryotic Translation Initiation Factor 2-3 | 4.86 | 103674_f_at | AJ006584 |
| Follistatin | 1.17 | 98817_at | Z29532 |
| GATA Binding Protein 6 | 1.90 | 104698_at | U51335 |
| Keratin Complex 2-8 | 1.76 | 101009_at | X15662 |
| Transmembrane 4 Superfamily 6 | 2.40 | 92555_at | AF053454 |
| Reversion Induced LIM | 1.41 | 104094_at | Y08361 |
| RAS 1 | 1.48 | 99032_at | AF009246 |
| S100 Calcium Binding Protein A13 | 2.23 | 100959_at | X99921 |
| FXYD Domain-containing Transport Regulator 3 | 2.05 | 103059_at | X93038 |
| Retinoic Acid A1 | 2.09 | 98320_at | Y12657 |
| Pleckstrin Homology-like Domain A3 | 1.59 | 98056_at | AI846214 |
| Clusterin | 2.35 | 95286_at | D14077 |
| Epiregulin | 1.89 | 98802_at | D30782 |
| Transgelin | 2.19 | 93541_at | Z68618 |
| Metallothionein 2 | 1.61 | 101561_at | K02236 |
| Metallothionein 1 | 2.09 | 93573_at | V00835 |
| Actin alpha 2 | 5.63 | 93100_at | X13297 |
| GRO1 Oncogene | 1.52 | 95349_g_at | J04596 |
| Serine Proteinase Inhibitor E1 | 2.15 | 94147_at | M33960 |
| Serine Protease 23 | 3.25 | 94238_at | AW228316 |
| Osteoblast Specific Factor 2 | 3.44 | 92593_at | D13664 |
| Serum-inducible Kinase | 1.42 | 92310_at | M96163 |
| Trophoblast Glycoprotein | 1.57 | 95345_at | AJ012160 |
| Lysyl Oxidase | 1.52 | 160095_at | D10837 |
| High Mobility Group AT-hook 2 | 2.23 | 99058_at | X99915 |
| Procollagen IV alpha 2 | 2.04 | 101039_at | X04647 |
| Glutathione S-transferase mu 2 | 1.63 | 93009_at | J04696 |
| Transient Receptor Protein 2 | 3.37 | 96939_at | AI842649 |
| Lectin 4 | 1.54 | 160099_at | AF026799 |

**Figure 3.** *Global expression changes of the transformation of teratocarcinoma cell from ES cells. (A) Cells in culture: a comparison of ESC versus TERC (P < .00005). Red indicates expression higher than the mean value. Green indicates expression below the mean value. Black indicates a value near the mean. Gene name is indicated to the right of the colored diagram. FC—fold change between the average expression values for the two groups being compared; Probe ID—Affymetrix probe identification number; Pub Acc—public accession number corresponding to the gene sequence used to generate the Affymetrix probe. (B) Tumors: a comparison of ES versus TER (P < .00005). Color scheme and labels identical to that described in Figure 4A.*

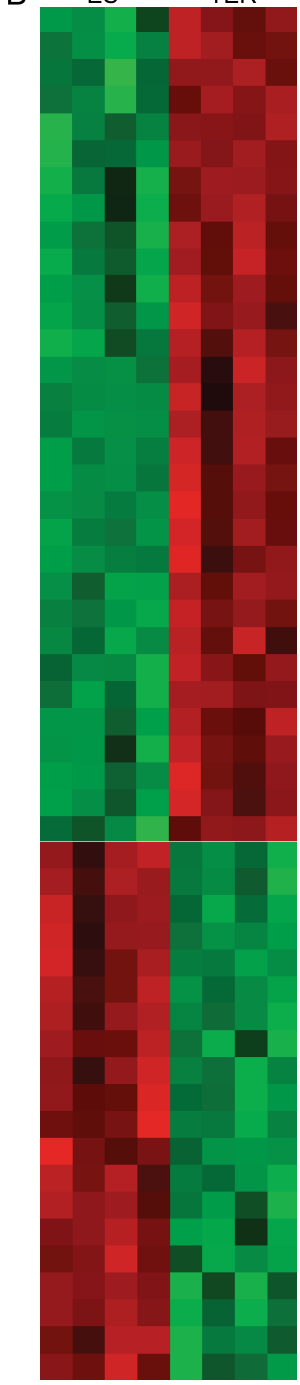


| Gene | FC | Probe ID | Pub Acc |
|---|---|---|---|
| hnRNP A2/B1 | 1.56 | 93117_at | AF073993 |
| Mesoderm Specific Transcript | 2.80 | 92607_at | AF017994 |
| Microfibrillar-associated 2 | 1.60 | 101095_at | L23769 |
| Zinc Finger Protein 143 | 1.31 | 102263_at | U29513 |
| Cell Division Cycle 25 | 1.87 | 102934_s_at | L16926 |
| Down-regulated in Metastasis | 1.09 | 104463_at | AI157789 |
| Cell Division Cycle 7 | 2.44 | 103797_at | AB019388 |
| Thyroid Hormone Receptor Interactor 13 | 3.19 | 101372_at | AI852645 |
| Rab 6 | 1.95 | 160501_at | Y09632 |
| HEC Protein | 2.92 | 93441_at | AI595322 |
| Serine/threonine Kinase 6 | 2.79 | 92639_at | U80932 |
| Centromere Protein E | 1.92 | 161076_at | AI462312 |
| Eukaryotic Translation Initiation Factor 1A/4C | 1.63 | 93358_at | AI836451 |
| Chromosomal Protein CAPC | 2.24 | 101906_at | AA032310 |
| Nucleolar Protein ANKT | 2.72 | 161000_i_at | AA275196 |
| Fibroblast Growth Factor Inducible 16 | 2.28 | 97421_at | U42385 |
| Ribonucleotide Reductase M2 | 2.54 | 102001_at | M14223 |
| Baculoviral IAP Repeat-containing 5 | 2.72 | 101521_at | AB013819 |
| Kinesin-like 1 | 4.00 | 99541_at | AJ223293 |
| Apoptosis Inhibitory Protein 5 | 1.32 | 101035_at | U35846 |
| Enhancer of Zeste 2 | 3.12 | 99917_at | U52951 |
| High Mobility Group Box 2 | 2.41 | 93250_r_at | X67668 |
| TEA Domain Family Member 2 | 1.34 | 96940_at | Y10026 |
| Pericentrin | 1.54 | 99662_at | AI194767 |
| DNA Polymerase alpha 1 | 2.26 | 103207_at | D13543 |
| Cell Division Cycle 6 | 2.69 | 103821_at | AJ223087 |
| Maternal Embryonic Leucine Zipper Kinase | 1.41 | 100416_at | L76158 |
| Checkpoint Kinase 1 | 1.62 | 103064_at | AF016583 |
| Nuclear Cap Binding Protein | 1.16 | 102400_at | AW125118 |
| TRAP 220 | 1.45 | 96577_i_at | AI853019 |
| Chromobox 3 | 1.32 | 100405_at | X56683 |
| Clusterin | 3.27 | 95286_at | D14077 |
| Small Proline-rich Protein 2G | 1.80 | 101754_f_at | AJ005565 |
| Keratin Complex 2-7 | 1.64 | 97920_at | AA755126 |
| FXYD-containing Ion Transport Regulator 2 | 1.39 | 94827_at | X70060 |
| SRY-box Containing 10 | 1.20 | 100283_at | AW125812 |
| Odorant Binding Protein IB | 1.34 | 101296_at | Y10972 |
| Tissue Inhibitor of Metalloproteinase 2 | 1.52 | 93507_at | X62622 |
| Endomucin | 1.63 | 94997_at | AF060883 |
| Insulin-like Growth Factor Binding Protein 6 | 1.69 | 103904_at | X81584 |
| Small Proline-rich Protein 1A | 1.47 | 160909_at | AF057156 |
| Uridine Phosphorylase | 1.40 | 104213_at | AI266885 |
| Norrie Disease Homolog | 1.32 | 92976_at | X92397 |
| S100 Calcium Binding Protein A1 | 1.94 | 95453_f_at | AF087687 |
| FXYD-containing Ion Transport Regulator 1 | 2.30 | 93040_at | AF091390 |
| A Disintegrin and Metalloprotease Domain 8 | 1.65 | 103024_at | X13335 |
| Serine Proteinase Inhibitor G1 | 1.46 | 99081_at | AF010254 |
| Eukaryotic Translation Initiation Factor 2-3 | 3.33 | 103674_f_at | AJ006584 |
| Insulin-like Growth Factor Binding Protein 7 | 1.48 | 160527_at | AB012886 |
| Serine Protease 23 | 1.89 | 94238_at | AW228316 |
| Calcyclin | 2.08 | 92770_at | X66449 |

**Figure 3.** *Continued.*

.001, so it is interesting to note that one gene, *trophoblast glycoprotein*, showed a contradictory expression pattern.

Trophoblast glycoprotein expression was seen to increase in the teratocarcinoma tumor compared to its expression in the teratocarcinoma cell line. This gene plays a role in the modulation of cell adhesion and mobility, which could explain the change in expression between the cell line and the tumor.

The other genes in the figure play key roles in a variety of cell cycle functions. CDC7 is critical for the initiation of DNA replication but also plays a role in maintenance of genomic integrity [8]. Mad2-like1 is involved in the cell cycle checkpoint responsible for appropriate spindle attachment to the centromere. Enhancer of Zeste 2 has histone methyl transferase activity. All of these genes are upregulated in both the teratocarcinoma cell line and in the tumor. Of the downregulated genes, *Clusterin* stands out. Its function is disputed but much of the evidence points to a proapoptotic role [9,10]. Two serine protease inhibitors, Cystatin C and Serine Proteinase Inhibitor G1, are downregulated as well.

In addition to the phenotypic response resulting from molecular changes during the transformation of the ES cells

A


| Gene | FC | Probe ID | Pub Acc |
|---|---|---|---|
| Testis Expressed 292 | 3.14 | 102315_at | AW124570 |
| Cell Division Control Protein CKS2 | 4.15 | 97527_at | AA681998 |
| Eukaryotic Translation Initiation Factor 2-2 beta | 3.59 | 97083_at | AA600468 |
| SRY-box Containing 17 | 5.86 | 92996_at | D49473 |
| Placentae and Embryos Oncofetal Gene | 14.94 | 101368_at | M32484 |
| Cell Division Cycle 2A | 3.71 | 100128_at | M38724 |
| KDEL Receptor 3 | 3.39 | 104464_s_at | AI642389 |
| Histone Acetyltransferase B | 3.87 | 97896_r_at | AW125218 |
| Metal Response Element Binding TF 2 | 3.81 | 102069_at | S78454 |
| Cyclin B1 | 4.54 | 160159_at | X64713 |
| Protein Regulator of Cytokinesis 1 | 3.91 | 95032_at | AA856349 |
| Eukaryotic Translation Initiation Factor 1A | 3.07 | 94745_f_at | U28419 |
| Geminin | 3.76 | 160069_at | AA681520 |
| DEAD/H Box 16 | 3.31 | 100559_at | AI853344 |
| HSPC150 | 5.00 | 100955_at | AA989957 |
| Ttk Protein Kinase | 3.98 | 103201_at | M86377 |
| Fibroblast Growth Factor Inducible 16 | 3.60 | 97421_at | U42385 |
| Teratocarcinoma-derived Growth Factor | 8.61 | 93002_r_at | M87321 |
| Nucleotide Binding Protein | 3.68 | 98948_at | AI785289 |
| Gap Junction Membrane Channel beta 5 | 4.90 | 104016_at | M91236 |
| Traf and Tnf Receptor Associated | 3.39 | 93538_at | AW228036 |
| MAD2-like 1 | 3.08 | 99632_at | U83902 |
| Embryonal Stem Cell Specific 1 | 17.04 | 160370_at | AA683849 |
| Cyclin F | 3.86 | 99073_at | Z47766 |
| POU Domain 5 Transcription Factor 1 | 14.50 | 103075_at | M34381 |
| Uridine-cytidine Kinase 2 | 4.20 | 94367_at | AI850362 |
| Heparan Sulfate 3-O-sulfotransferase 1 | 7.17 | 102410_at | AF019385 |
| FBJ Osteosarcoma Oncogene | 5.14 | 160901_at | V00727 |
| Syntaxin 3 | 3.77 | 100499_at | D29797 |
| GATA 6 | 3.93 | 104698_at | U51335 |
| Thyroid Hormone Receptor Interactor 13 | 4.91 | 101372_at | AI852645 |
| Highly Expressed in Cancer | 4.99 | 93441_at | AI595322 |
| Cell Division Cycle 6 | 4.41 | 103821_at | AJ223087 |
| Serine/threonine Kinase 6 | 4.94 | 92639_at | U80932 |
| Undifferentiated Embryonic Cell TF 1 | 4.19 | 102220_at | AB017360 |
| Early Growth Response 1 | 4.57 | 98579_at | M28845 |
| Testis Expressed 19 | 7.97 | 102418_at | AA793009 |
| Disabled 2 | 5.33 | 98045_s_at | U18869 |
| GRO1 Oncogene | 14.17 | 95348_at | J04596 |
| High Mobility Group AT-hook 2 | 8.75 | 99058_at | X99915 |
| Epiregulin | 5.02 | 98802_at | D30782 |
| Cysteine Rich 61 | 3.48 | 92777_at | M32490 |
| Heat Shock Protein 2 | 4.15 | 99816_at | M20567 |
| Forkhead Box A1 | 8.26 | 92697_at | U44752 |
| Prominin | 61.12 | 93389_at | AF039663 |
| Insulin-like Growth Factor BP 7 | 6.11 | 160527_at | AB012886 |
| Cathepsin S | 16.76 | 98543_at | AJ223208 |
| 2,3-bisphosphoglycerate Mutase | 6.72 | 94815_at | X13586 |
| Osteoblast Specific Factor 2 | 6.72 | 92593_at | D13664 |
| Clusterin | 4.68 | 95286_at | D14077 |
| Cofilin 2 | 3.77 | 97549_at | L29468 |
| Lysozyme | 51.64 | 100611_at | M21050 |
| Endomucin | 3.53 | 94997_at | AF060883 |
| Sorbin and SH3 Domain Containing 1 | 6.68 | 160320_at | U58883 |
| Secretogranin III | 34.06 | 162237_f_at | AV328553 |
| Tetranectin | 4.86 | 92224_at | X79199 |
| Carboxypeptidase E | 3.60 | 99643_f_at | X61232 |
| Microfibrillar-associated 2 | 3.11 | 101095_at | L23769 |
| E26 Avian Leukemia Oncogene 1 | 3.74 | 94720_at | M58482 |
| Lung Carcinoma Myc Related Oncogene 1 | 4.12 | 102235_at | X13945 |
| Thymosin B4 | 3.18 | 96426_at | U38967 |
| Cysteine Rich 2 | 6.19 | 101593_at | AI851454 |
| Steroid Sensitive 1 | 5.83 | 160298_at | AW122012 |
| Hsp40 B10 | 3.25 | 98451_at | AI843164 |

**Figure 4.** *An examination of the expression changes associated with the transition from in vitro to in vivo. (A) The expression of genes in ES cells in culture compared to the expression of genes in ES cell tumors induced in nude mice (P < .001). Labeling and color scheme identical to that described in (A). (B) The expression of genes in teratocarcinoma cells in culture compared to teratocarcinomas induced in nude mice. Labeling and color scheme identical to that described in (A).*

B


| Gene | FC | Probe ID | Pub Acc |
|---|---|---|---|
| Peter Pan | 3.37 | 161016_at | AA673574 |
| Chemokine Orphan Receptor 1 | 4.75 | 93430_at | AF000236 |
| Cysteine Dioxygenase 1 | 3.95 | 96346_at | AI854020 |
| Transmembrane 4 Superfamily 2 | 4.64 | 93326_at | D26483 |
| Microsomal Glutathione S-transferase 1 | 7.93 | 93026_at | AW124337 |
| Cadherin 5 | 6.84 | 104083_at | AI853217 |
| BCL2 Related Protein A1D | 2.92 | 93869_s_at | U23781 |
| Lysozyme | 75.94 | 100611_at | M21050 |
| Open Reading Frame 12 | 5.00 | 99191_at | AI844939 |
| SH3-binding Domain Glutamic Acid-rich | 4.31 | 93806_at | AI848671 |
| Ligand of Numb X 1 | 4.89 | 102038_at | AF034745 |
| SRY-box Containing 11 | 5.89 | 101631_at | AF009414 |
| MARCKS | 8.96 | 96865_at | M60474 |
| Neuropilin | 4.89 | 95016_at | D50086 |
| Paternally Expressed 3 | 7.01 | 161316_f_at | AV353105 |
| Hepatocellular Carcinoma-associated 112 | 3.82 | 96605_at | AI787183 |
| Prostate Tumor Over Expressed 1 | 3.18 | 99599_s_at | AW210320 |
| Nuclear Factor I/B | 5.68 | 99440_at | Y07686 |
| Mesoderm Specific Transcript | 5.00 | 92607_at | AF017994 |
| ERp72 | 3.46 | 99645_at | AW048484 |
| SWI/SNF related E1 | 3.76 | 96651_at | AF035263 |
| Retinol Binding Protein 4 | 4.82 | 96047_at | U63146 |
| Drebrin 1 | 5.83 | 103430_at | AW124952 |
| Rho B | 3.14 | 101030_at | X99963 |
| Pleiomorphic Adenoma-like 1 | 9.84 | 92502_at | X95504 |
| Nestin | 7.45 | 103549_at | AW061260 |
| Zinc Finger of the Cerebellum 1 | 6.92 | 104169_at | D32167 |
| Transient Receptor 2 | 14.14 | 96939_at | AI842649 |
| Microfibrillar-associated 2 | 4.89 | 101095_at | L23769 |
| Insulin-like Growth Factor BP 7 | 5.57 | 160527_at | AB012886 |
| Immediate Early Response 5 | 6.82 | 92773_at | AF079528 |
| Leucine Rich Repeat 1 | 3.34 | 161045_at | D45913 |
| Membrane-spanning 4-domains A-6B | 6.45 | 102104_f_at | AI504305 |
| Transgelin | 3.90 | 93541_at | Z68618 |
| Placentae and Embryos Oncofetal Gene | 4.39 | 101368_at | M32484 |
| Uridine Phosphorylase | 5.23 | 100030_at | D44464 |
| Laminin alpha 1 | 5.57 | 103729_at | M36775 |
| Secretory Proteoglycan | 3.60 | 94085_at | M34603 |
| N-acetylneuraminate Pyruvate Lyase | 3.80 | 94330_at | AA710564 |
| Teratocarcinoma-derived Growth Factor | 10.44 | 93002_r_at | M87321 |
| Kruppel-like Factor 4 | 4.90 | 99622_at | U20344 |
| Fatty Acid Binding Protein 3 | 5.43 | 94214_at | X14961 |
| Metal Response Element Transcription Factor 2 | 3.25 | 102069_at | S78454 |
| Makorin 1 | 3.87 | 101069_g_at | AA656621 |
| Embryonal Stem Cell Specific 1 | 5.00 | 160370_at | AA683849 |
| Undifferentiated Embryonic Cell TF 1 | 4.22 | 102220_at | AB017360 |
| Solute Carrier 2-3 | 3.54 | 93804_at | AI854156 |
| POU Domain 5 Transcription Factor 1 | 5.09 | 103075_at | M34381 |
| Glycosylasparaginase | 3.44 | 97154_f_at | AA413015 |
| Amyotrophic Lateral Sclerosis 2 | 3.34 | 96900_at | AW125480 |
| Solute Carrier 29-1 | 3.28 | 95733_at | AI838274 |
| Laminin B1-1 | 3.44 | 101948_at | X05212 |
| Telomeric Repeat Binding Factor 1 | 3.07 | 99920_at | U65586 |
| Disabled 2 | 4.91 | 98045_s_at | U18869 |
| Low Density Lipoprotein Receptor-related 2 | 4.87 | 103377_at | AW259788 |
| HSPC150 | 3.51 | 100955_at | AA989957 |
| T-box 3 | 6.31 | 103538_at | AW121328 |
| Lectin 2 | 4.52 | 160221_at | AA709879 |
| Tumor-associated Calcium Signal Transducer 1 | 3.05 | 99582_at | M76124 |

**Figure 4.** *Continued.*

into teratocarcinoma cells, we recognize the potential for drastic change in gene expression during the transition from culture to *in vivo* (see Figure 4). Figure 6*B* details those genes whose expression changes are common between the cell cultures and tumors of both the ES cells and the teratocarcinomas.

There are seven genes that are downregulated in both the ES cell and teratocarcinoma tumors. Included in the list of genes with decreased expression after tumor induction are genes specifically involved in the maintenance of the embryonal nature of the cells: PEM, undifferentiated embryonal cell TF 1, embryonal stem cell–specific 1, and,

surprisingly, teratocarcinoma-derived growth factor. Interestingly, Disabled 2, shown to be involved in the MAPK pathway [11] and to mediate c-fos expression and the cell growth–regulatory function of retinoic acid in F9 embryonic stem cell–like teratocarcinoma cells [12], is also downregulated in the tumors. Metal response element binding transcription factor 2 and POU domain 5 transcription factor 1 are also downregulated in the tumors.

There are three genes that are upregulated in both tumor types. Those genes with increased expression in the tumors are lysozyme, microfibrillar-associated 2, and insulin-like growth factor binding protein 7. The upregulation of microfibrillar-associated 2, shown to interact with fibrillin-1 and fibrillin-2 [13], may result from the need to establish an anchor for growth in the host. Insulin-like growth factor binding protein 7/mac25 has been shown to be downregulated in liver tumorigenesis [14], but in our system, this factor seems to have a positive growth influence.

To identify the precise genes or pathways responsible for teratocarcinoma induction, altered gene expression in teratocarcinomas was investigated. Microarray, together with the GenMAPP analysis, revealed that several cellular pathways are involved in the teratocarcinoma tumorigenesis, possibly through the interplay among cell cycle regulation, apoptosis, G13 pathway, TGFβ pathway, and Wnt pathway. GenMapp showed that a total of 26 genes have altered with fold change of ±1.5 in the cell cycle pathway. Out of these 26 genes, 19 have the *P* value ≤.05 (Figure 7). The expression of the following genes in cell cycle pathway—mitotic checkpoint serine/threonine protein kinase (*BUB1*), mitotic spindle assembly checkpoint protein (*MAD2L1*), M-phase inducer phosphatase 3 (*Cdc25A*), E-cadherin (*Cdh1*), G2/mitotic-specific cyclin B1 (*CycB1*), cell division control protein 2 homolog (*CDK1*), Wee1-like protein kinase (*WEE1*), cell division cycle 7–related protein kinase (*Cdc7*), transcription factor DP-1 (*DP1*), cell division protein kinase 4 (*CDK4*), DNA replication licensing factors (*MCM2*, *MCM3*, *MCM4*,

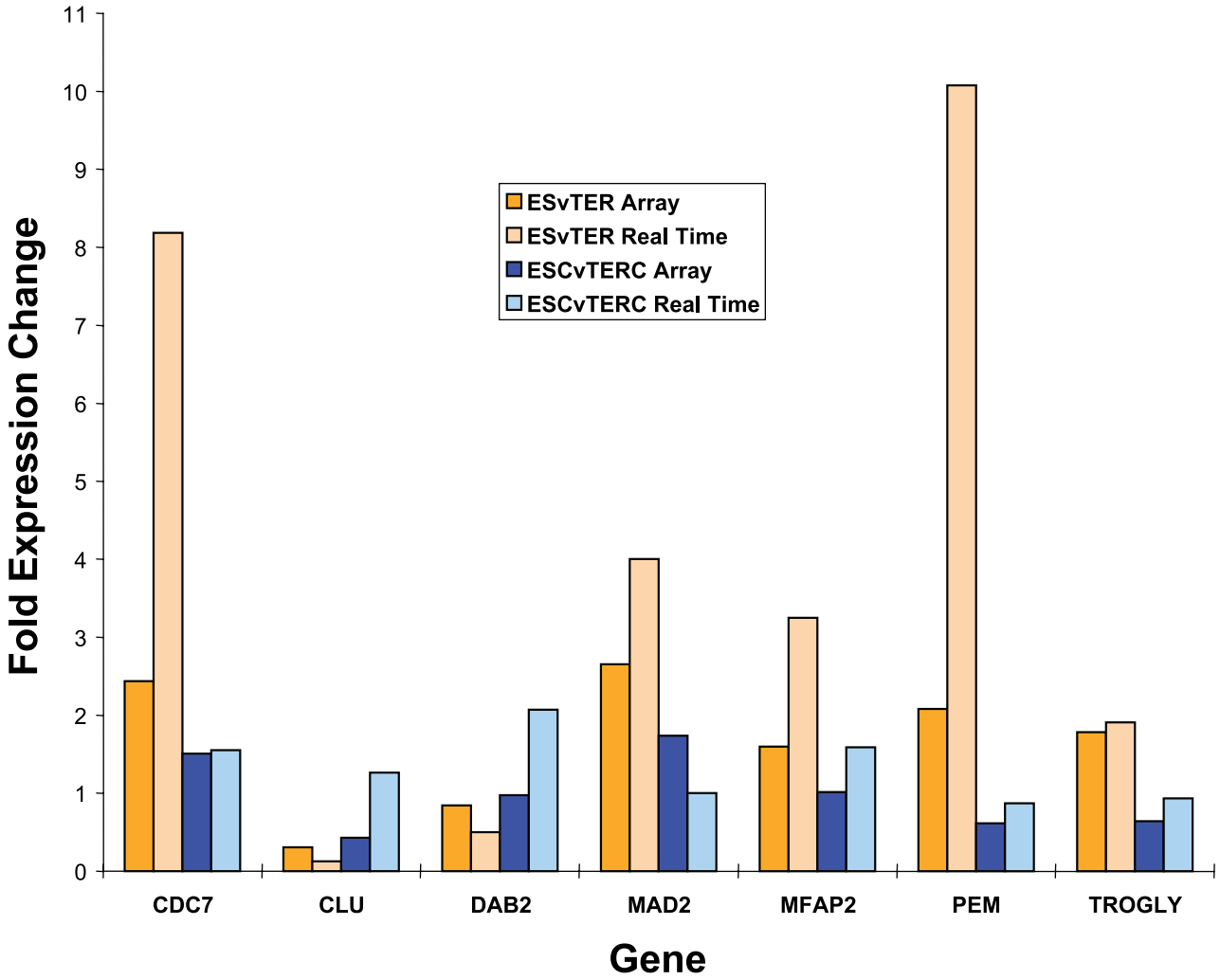


**Figure 5.** *Real-time RT-PCR analysis of several genes of interest compared to the microarray expression analysis. ES cell tumor data (ES) are compared to teratocarcinoma data (TER) for both microarray data (dark orange) and real-time RT-PCR (light orange). Also included are data from the ES cell culture (ESC) versus teratocarcinoma cell culture (TERC) for both microarray data (dark blue) and real-time RT-PCR data (light blue). Gene name is on the X-axis and fold change is on the Y-axis. Real-time PCR was performed on two samples and the value presented is the average of the two samples (with a variation of less than 10%).*

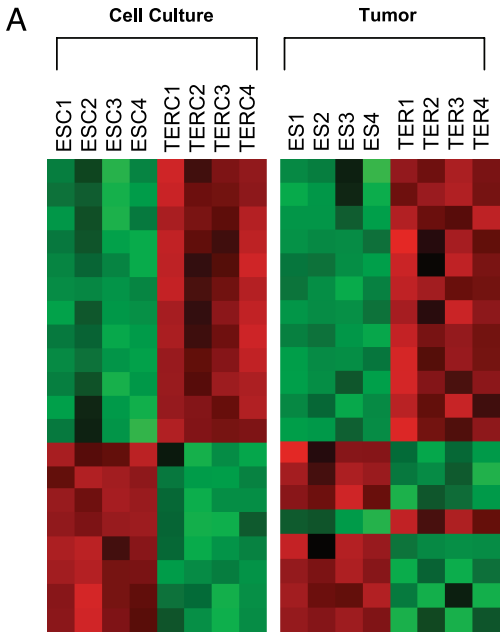


| Gene | FCC | FCT | Probe ID | Pub Acc |
|---|---|---|---|---|
| Nonsense mRNA Reducing Factor 1 | 1.27 | 1.41 | 103444_at | AI272489 |
| Cell Division Cycle 7 | 2.17 | 2.54 | 103797_at | AB019388 |
| DNA Polymerase alpha 1 | 1.58 | 1.75 | 103207_at | D13543 |
| MAD2-like 1 | 1.42 | 1.62 | 99632_at | U83902 |
| U6 snRNA-associated Sm-like Protein 8 | 1.53 | 2.26 | 102409_at | AW046963 |
| Mesoderm Specific Transcript | 1.30 | 1.87 | 92607_at | AF017994 |
| Eukaryotic Translation Initiation Factor 1A | 4.86 | 3.33 | 93358_at | AI836451 |
| Enhancer of Zeste 2 | 1.51 | 2.44 | 99917_at | U52951 |
| Ribonucleotide Reductase M2 | 1.58 | 1.50 | 102001_at | M14223 |
| Checkpoint Kinase 1 | 1.52 | 4.86 | 103064_at | AF016583 |
| High Mobility Group Box 2 | 2.51 | 2.80 | 93250_r_at | X67668 |
| Maternal Embryonic Leucine Zipper Kinase | 1.40 | 2.41 | 100416_at | L76158 |
| Low Density Lipoprotein Receptor 8 | 1.56 | 1.63 | 96605_at | AI787183 |
| Clusterin | 3.25 | 1.89 | 95286_at | D14077 |
| Serine Protease 23 | 2.35 | 3.27 | 94238_at | AW228316 |
| Trophoblast Glycoprotein | 1.57 | 1.78 | 95345_at | AJ012160 |
| Keratin Complex 1 Gene 19 | 1.61 | 1.82 | 92550_at | M36120 |
| Eukaryotic Translation Initiation Factor 2 S3Y | 1.51 | 1.46 | 103674_f_at | AJ006584 |
| Cystatin C | 1.73 | 2.65 | 161522_i_at | AV218205 |
| Serine (or cysteine) Proteinase Inhibitor G1 | 2.01 | 3.12 | 99081_at | AF010254 |

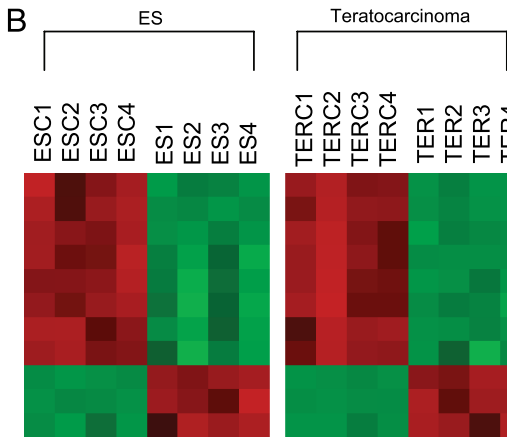


| Gene | FC ES | FC T | Probe ID | Pub Acc |
|---|---|---|---|---|
| Placentae and Embryos Oncofetal Gene | 14.94 | 4.39 | 101368_at | M32484 |
| Metal Response Element Binding TF 2 | 3.81 | 3.25 | 102069_at | S78454 |
| Undifferentiated Embryonic Cell TF 1 | 4.19 | 4.22 | 102220_at | AB017360 |
| POU Domain 5 Transcription Factor 1 | 14.50 | 5.09 | 103075_at | M34381 |
| Embryonal Stem Cell Specific 1 | 17.04 | 5.00 | 160370_at | AA683849 |
| Teratocarcinoma-derived Growth Factor | 8.61 | 10.44 | 93002_r_at | M87321 |
| Disabled 2 | 5.33 | 4.91 | 98045_s_at | U18869 |
| Lysozyme | 51.64 | 75.94 | 100611_at | M21050 |
| Microfibrillar-associated 2 | 3.11 | 4.89 | 101095_at | L23769 |
| Insulin-like Growth Factor BP 7 | 6.11 | 5.57 | 160527_at | AB012886 |

**Figure 6.** *(A) Similarities between the expression patterns of genes with differential expression between ES cell culture and teratocarcinoma cell culture, as well as ES cell tumor and teratocarcinoma. Labeling and color scheme identical to that described in Figure 4A. FCC—fold change between the average expression values for ES cells versus the teratocarcinoma cells in culture; FCT—fold change between the average expression values for ES cell tumors versus teratocarcinomas. (B) Similarities between the expression patterns of genes with differential expression between the cell cultures and the tumors for both the ES cell and the teratocarcinoma cells. Labeling and color scheme identical to that described in Figure 4A. FC ES—fold change between the average expression values for ES cell cultures versus the ES cell tumors. FCT—fold change between the average expression values for teratocarcinoma cell cultures versus the teratocarcinomas.*

*MCM5*, and *MCM7*), and E2F5—is found to be altered in the teratocarcinomas. For example, cell cycle proteins regulate multiple cell type–dependent cell cycle–regulating events, including cell cycle checkpoint enforcement and regulating exit from mitosis and normal mitotic timing (BUB1), mitotic checkpoint (MAD2L1), progression of the cell cycle (CDC25A), control of cell cycle at the G2/M (mitosis) transition (CycB1, CDK1, WEE1, and Cdc7), and cell cycle progression from G1 to S phase (DP1, MCM2, MCM3, MCM5, MCM7, and E2F5). Crosstalk of these cellular processes may be involved in the teratocarcinoma tumorigenesis. Although the exact molecular mechanism behind the development of teratocarcinoma is still not clear, our data show that several dysregulated cellular signaling pathways, especially the cell cycle pathway, are important in this malignancy.

In summary, this study of teratocarcinoma tumorigenesis has provided clues underlying the transformation of embryonic stem cells and has found that no gross cytogenetic changes occurred in this type of cancer formation. We have also presented gene expression changes specific to the transition from *in vitro* to *in vivo*.

## References

[1] Mintz B and Fleischman RA (1981). Teratocarcinomas and other neoplasms as developmental defects in gene expression. *Adv Cancer Res* **34,** 211–278.

[2] Stevens LC (1970). The development of transplantable teratocarcinomas from intratesticular grafts of pre- and postimplantation mouse embryos. *Dev Biol* **21,** 364–382.

[3] Lockhart DJ, Dong H, Byrne MC, Follettie MT, Gallo MV, Chee MS, Mittmann M, Wang C, Kobayashi M, Horton H, and Brown EL (1996).

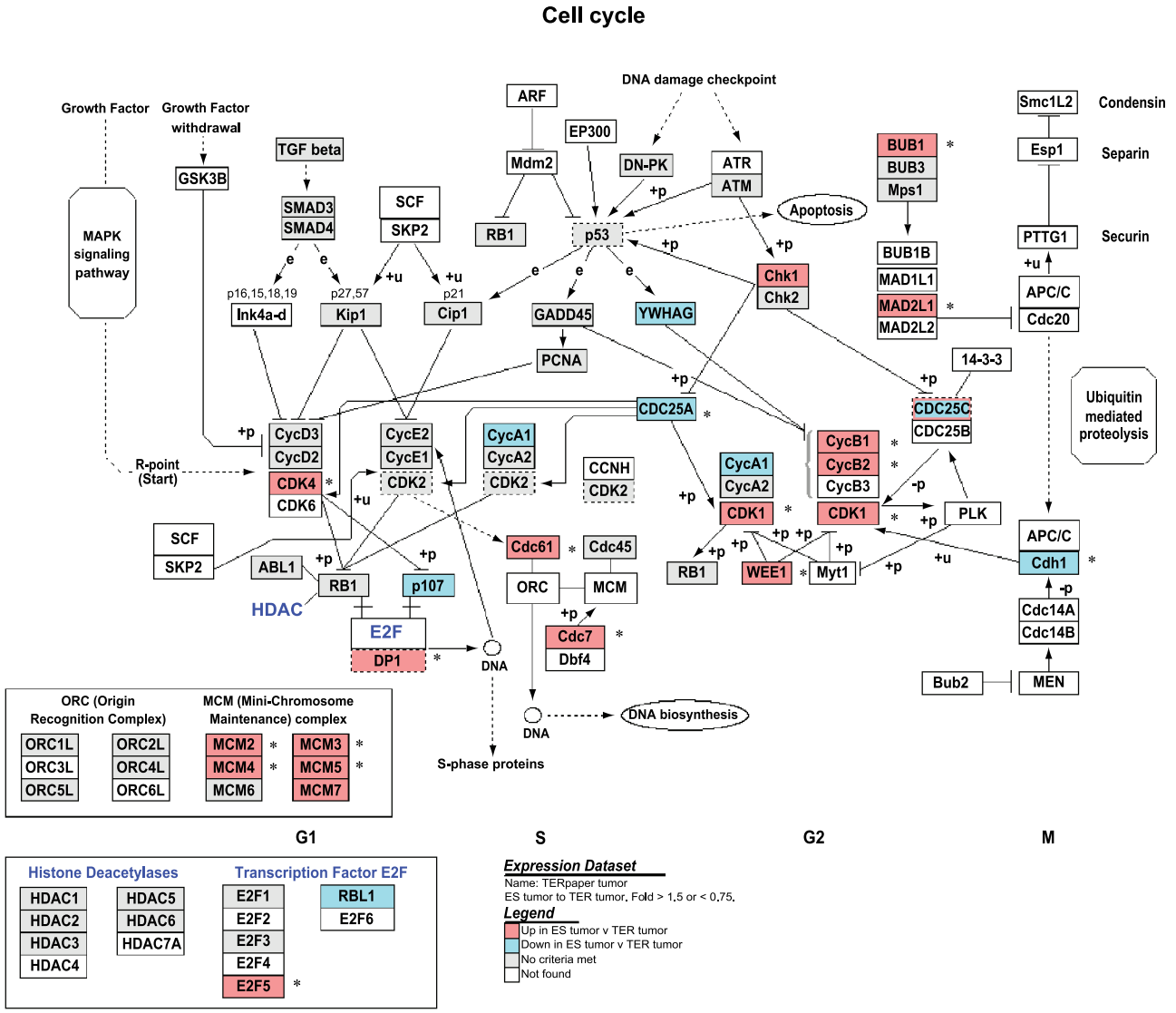


**Figure 7.** *GenMAPP Cell cycle pathways integrating our expression data (cutoff: fold change >1.5 or < 0.75 in ES tumors versus TER tumors). Red indicates overexpressed genes in ES tumors. Blue indicates overexpressed genes in TER tumors. Grey indicates that the selection criteria were not met but the gene is represented on the array. White boxes indicate that the gene was not present on the chip. *The gene has fold change >1.5 or <0.75 in ES tumors versus TER tumors with $P \leq .05$.*

Expression monitoring by hybridization to high-density oligonucleotide arrays. *Nat Biotechnol* **14** (**13**), 1675–1680.

[4] Wodicka L, Dong H, Mittmann M, Ho MH, and Lockhart DJ (1997). Genome-wide expression monitoring in *Saccharomyces cerevisiae*. *Nat Biotechnol* **15** (**13**), 1359–1367.

[5] Lemon WJ, Palatini JJ, Krahe R, and Wright FA (2002). Theoretical and experimental comparisons of gene expression indexes for oligonucleotidearrays. *Bioinformatics* **18** (**11**), 1470–1476.

[6] Li C and Wong WH (2001). Model-based analysis of oligonucleotide arrays: expression index computation and outlier detection. *Proc Natl Acad Sci USA* **98** (**1**), 31–36.

[7] Dahlquist KD, Salomonis N, Vranizan K, Lawlor SC, and Conklin BR (2002). GenMAPP, a new tool for viewing and analyzing microarray data on biological pathways. *Nat Genet* **31** (**1**), 19–20.

[8] Jares P, Donaldson A, and Blow JJ (2000). The Cdc7/Dbf4 protein kinase: target of the S phase checkpoint? *EMBO Rep* **1** (**4**), 319–322.

[9] Park JH, Park JS, Ju SK, Lee KB, Park YK, Kang MH, Na SY, and You KH (2003). Clusterin mRNA expression in apoptotic and activated rat thymocytes. *Cell Res* **13** (**1**), 49–58.

[10] Leskov KS, Klokov DY, Li J, Kinsella TJ, and Boothman DA (2003). Synthesis and functional analyses of nuclear clusterin, a cell death protein. *J Biol Chem* **278** (**13**), 11590–11600.

[11] Tseng CP, Huang CH, Tseng CC, Lin MH, Hsieh JT, and Tseng CH (2001). Induction of disabled-2 gene during megakaryocyte differentiation of k562 cells. *Biochem Biophys Res Commun* **285** (**1**), 129–135.

[12] Smith ER, Capo-chichi CD, He J, Smedberg JL, Yang DH, Prowse AH, Godwin AK, Hamilton TC, and Xu XX (2001). Disabled-2 mediates c-Fos suppression and the cell growth regulatory activity of retinoic acid in embryonic carcinoma cells. *J Biol Chem* **276** (**50**), 47303–47310.

[13] Penner AS, Rock MJ, Kielty CM, and Shipley JM (2002). Microfibril-associated glycoprotein-2 interacts with fibrillin-1 and fibrillin-2 suggesting a role for MAGP-2 in elastic fiber assembly. *J Biol Chem* **277** (**38**), 35044–35049.

[14] Komatsu S, Okazaki Y, Tateno M, Kawai J, Konno H, Kusakabe M, Yoshiki A, Muramatsu M, Held WA, and Hayashizaki Y (2000). Methylation and downregulated expression of mac25/insulin-like growth factor binding protein-7 is associated with liver tumorigenesis in SV40T/t antigen transgenic mice, screened by restriction landmark genomic scanning for methylation (RLGS-M). *Biochem Biophys Res Commun* **267** (**1**), 109–117.